MOF Catalysis

International Edition: DOI: 10.1002/anie.201712818
German Edition: DOI: 10.1002/ange.201712818

A Chromium Hydroxide/MIL-101(Cr) MOF Composite Catalyst and Its Use for the Selective Isomerization of Glucose to Fructose

Qiang Guo, Limin Ren, Prashant Kumar, Viktor J. Cybulskis, K. Andre Mkhoyan, Mark E. Davis, and Michael Tsapatsis**

Abstract: *A metal–organic framework (MOF)-based catalyst, chromium hydroxide/MIL-101(Cr), was prepared by a one-pot synthesis method. The combination of chromium hydroxide particles on and within Lewis acidic MIL-101 accomplishes highly selective conversion of glucose to fructose in the presence of ethanol, matching the performance of optimized Sn-containing Lewis acidic zeolites. Differently from zeolites, NMR spectroscopy studies with isotopically labeled molecules demonstrate that isomerization of glucose to fructose on this catalyst, proceeds predominantly via a proton transfer mechanism.*

Metal–organic frameworks (MOFs) are a class of crystalline materials with high surface areas and well-defined pore systems that hold promise for uses as adsorbents and membranes.[1–7] The ability to tune their composition also provides opportunities in heterogeneous catalysis, especially when bifunctional catalysts are desirable, such as in the catalysis of tandem reactions.[7–26] One such reaction is the isomerization of glucose to fructose in the presence of alcohols.[27–30] First proposed by Saravanamurugan et al.,[27] it has been shown to be a high-yield route to fructose and a promising alternative to aqueous routes. For instance, when glucose isomerization to fructose is combined with fructose ketalization, increased fructose yields beyond the equilibrium levels are achievable and the obtained fructoside is readily hydrolyzed to fructose upon addition of water (Scheme 1).

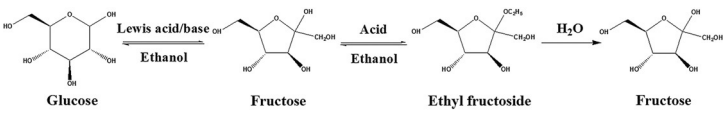

Scheme 1. Conversion of glucose to fructose in ethanol and water through sequential reactions.

[*] Dr. Q. Guo, Dr. L. Ren, P. Kumar, Prof. K. A. Mkhoyan, Prof. M. Tsapatsis
Department of Chemical Engineering and Materials Science
University of Minnesota
421 Washington Ave SE, Minneapolis, MN 55455 (USA)
E-mail: lren@umn.edu
tsapatsis@umn.edu
Dr. V. J. Cybulskis, Prof. M. E. Davis
Chemical Engineering, California Institute of Technology
Pasadena, CA 91125 (USA)
Supporting information and the ORCID identification number(s) for the author(s) of this article can be found under: https://doi.org/10.1002/anie.201712818.

MOF catalysts have been explored for glucose isomerization in water and recently their performance has approached that of the best zeolite catalysts (Sn-Beta).[31–33] Although a MOF-derived catalyst has been explored for glucose isomerization in alcohol, its performance was below that obtained by zeolite catalysts, such as Sn-SPP.[34] Herein, we demonstrate that a chromium hydroxide/MIL-101 catalyst can isomerize glucose to fructose at glucose conversion and fructose yield comparable to those obtained by optimized zeolite catalysts. We also show that the isomerization mechanism is predominantly by proton-transfer as in base-catalyzed isomerization, possibly due to chromium hydroxide, while the ketalization reaction is catalyzed by MIL-101. To our knowledge, this work is the first demonstration of a base-like, proton-transfer dominated, high yield catalytic route for fructose by glucose isomerization.

We observed that by increasing the amount of the amino acid glycine (GLY) in a MIL-101 synthesis mixture, increased amounts of co-precipitated $Cr(OH)_3$ nanoparticles were obtained. Figures 1 A–C show the results obtained from syntheses with composition (molar ratio): 1.0 Cr: 0.8 terephthalic acid (BDC): 265 H_2O: x GLY, where $x = 1.6$, 1.3, and 1.0. We also determined that the $Cr(OH)_3$ particles formed after the nucleation and initial crystal growth of MIL-101, and that in the absence of BDC linkers, nearly carbon-free particles are obtained which we call $Cr(OH)_3$-[GLY] (Figure 1 E, Figure S1D and Table S1 in the Supporting Information). The crystal structure of $Cr(OH)_3$ is not precisely known and a comparison of $Cr(OH)_3$-[GLY] with the typical XRD of $Cr(OH)_3$ provided in Figure 1 E indicates that $Cr(OH)_3$-[GLY] is a nanocrystalline material with distinct structure from $Cr(OH)_3$ made by precipitation at room temperature.[35] When using the composition 1.0 Cr: 0.8 BDC: 265 H_2O: 0.8 GLY, we obtained MIL-101 crystals with $Cr(OH)_3$ particles attached to and embedded in their periphery (Figure 1 D). These $Cr(OH)_3$ particles could not be separated by repeated sonication and washing. This Cr-$(OH)_3$/MIL-101(Cr) material is denoted from now on as MIL-101-[GLY]. We also prepared, for reference, three other Cr-MIL-101 catalysts: MIL-101-HF, MIL-101 and MIL-101-nano (Figure S1 and additional details for the materials synthesis can be found in the Supporting Information). XRD data of MIL-101-[GLY] show the characteristic reflections of MIL-101 along with reflection attributed to $Cr(OH)_3$ (Figure 1 E and Figure S1D). The broad Bragg reflections of the XRD pattern could be attributed to the small particle size. TEM images show that the particle size of MIL-101-[GLY] is around 80 nm, which is smaller than that of the MIL-101

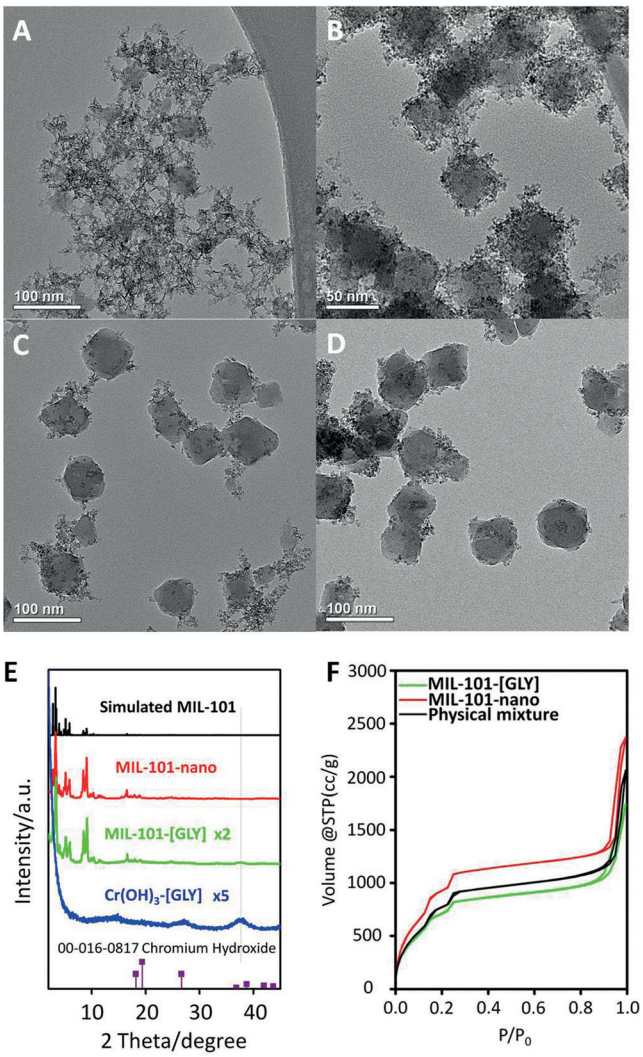

Figure 1. TEM images of materials prepared using 1.0 Cr:0.8 BDC:265 H_2O:*x* GLY with $x = 1.6$ (A), 1.3 (B), 1.0 (C), and 0.8 (D); XRD patterns (E) of simulated MIL-101, MIL-101-nano, MIL-101-[GLY], $Cr(OH)_3$-[GLY], and $Cr(OH)_3$ from JCPDS card No. 00-016-0817; Ar sorption isotherms (F) of MIL-101-nano, MIL-101-[GLY], and a physical mixture of 83 wt% MIL-101-nano and 17 wt% $Cr(OH)_3$-[GLY].

synthesized without glycine. The argon adsorption isotherm of the MIL-101-[GLY] shows two uptake steps around $P/P_0 = 0.1$ and $P/P_0 = 0.2$, which indicate the existence of two different windows in the framework, and the pore size distribution reflects two kinds of pore sizes centered at 2.2 and 2.9 nm.[36] Its BET equivalent surface area is lower than that of the nano-sized MIL-101 (MIL-101-nano) (2609 $m^2 g^{-1}$ versus 3661 $m^2 g^{-1}$) due to the presence of $Cr(OH)_3$. The surface area (2970 $m^2 g^{-1}$) of a physical mixture (ratio determined by Cr content calibration with MIL-101-[GLY], Table S1) of MIL-101-nano (83 wt%) and $Cr(OH)_3$-[GLY] (17 wt%) is comparable to that of the MIL-101-[GLY] (Figure 1F). IR spectra of deuterated acetonitrile adsorbed on MIL-101-[GLY] exhibit two bands at 2260 and 2311 cm^{-1} (Figure S2). The band at 2260 cm^{-1} can be assigned to the physisorbed deuterated acetonitrile and the band at 2311 cm^{-1} arises from the deuterated acetonitrile adsorption on Lewis acid sites.[21,37] With increasing temperature, the band at 2260 cm^{-1} vanished while the band at 2311 cm^{-1} remained unchanged indicating that the MIL-101-[GLY] shows strong Lewis acidity.

MIL-101-[GLY] was used as the catalyst for glucose isomerization/fructose ketalization in ethanol followed by fructoside hydrolysis in water (Scheme 1) and its performance was compared to that of several other MIL-101 materials. In the first step of this approach (first introduced in Ref. [27]), glucose is isomerized to fructose and fructose reacts with ethanol to give a mixture of fructose and ethyl fructoside. Then, water is added and hydrolysis of the fructoside yields fructose. Table 1 shows glucose conversion and product yield from different MOF catalysts. The fructose yields on MIL-101-HF, MIL-101 and MIL-101-nano are 20.2%, 24.3% and 24.9%, respectively, after 24 h reactions at 100 °C. Remarkably, 59.3% yield of fructose was obtained by using MIL-101-[GLY] at the same conditions.

Table 1: Glucose isomerization catalyzed by MOFs.[a]

Entry	Catalyst	Conv. [%][b]	Product yield [%][c]			Ref.
			FRU	MAN	HMF	
1	MIL-101-HF	33.6	20.2	3.6	0.8	This work
2	MIL-101	39.4	24.3	4.3	1.0	This work
3	MIL-101-nano	46.2	24.9	5	1.2	This work
4	MIL-101-[GLY]	76.5	59.3	2.9	1.4	This work
5	$Cr(OH)_3$-[GLY]	48.8	24.3	3.2	1.1	This work
6	Physical mixture[d]	60.4	37.4	4.1	1.2	This work
7	NU-1000 derived oxide	52.5	23.4	–	–	Ref. [34]
8	MIL-101-SO_3H in water	22	21.6	–	–	Ref. [31]
9	UiO-66 in water	31	ca. 22	–	ca. 6	Ref. [32]
10	Sn-Beta in water	59	32	9	–	Ref. [33]

[a] Reaction conditions: 1 wt% glucose (0.036 g) in ethanol (3.564 g) at 100 °C for 24 h, 0.013 wt% (based on Cr) catalyst. After quenching the reactor, 4.8 g of deionized water was added to perform the hydrolysis at 100 °C for 24 h. [b] Glucose conversion. [c] FRU: fructose; MAN: mannose; HMF: 5-hydroxymethylfurfural. [d] 83 wt% MIL-101-nano and 17 wt% $Cr(OH)_3$-[GLY].

Figure 2 shows the structure (as revealed by ADF-STEM) and corresponding isomerization performance of MIL-101-[GLY], MIL-101-nano and $Cr(OH)_3$-[GLY] catalysts. The ADF-STEM images of MIL-101-[GLY] match well with the corresponding atomic structure models when viewed along different directions (Figure S3). The bright contrast features (Figure 2A,B) in the images are $Cr(OH)_3$ nanoparticles grown both on and inside the outer parts of MIL-101 crystals. In the presence of MIL-101-[GLY], about 60% yield of fructose was obtained at 76.5% glucose conversion after 24 h of reaction (Figure 2C). The profile of fructose yield vs. glucose conversion on MIL-101-[GLY] is very similar to that

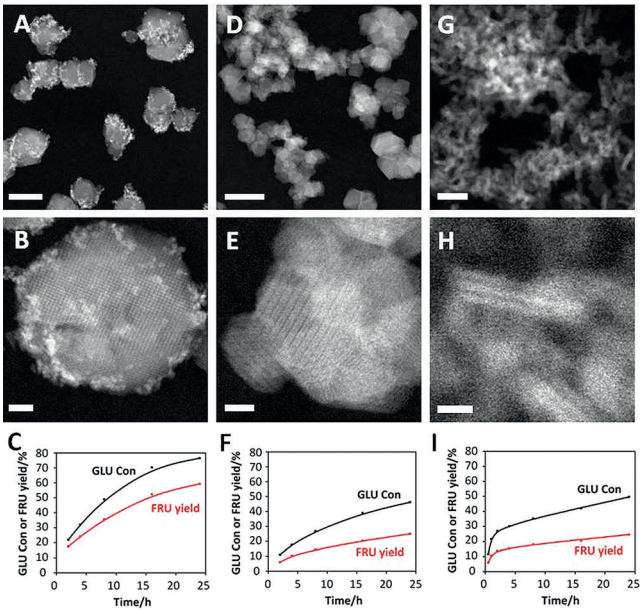

Figure 2. High-resolution ADF-STEM images and glucose (GLU) isomerization to fructose (FRU) profiles for A)–C) MIL-101-[GLY], D)–F) MIL-101-nano, and G)–I) $Cr(OH)_3$-[GLY]. Reaction conditions: 1 wt% glucose (0.036 g) in ethanol (3.564 g) at 100 °C, 0.013 wt% (based on Cr) catalyst. After quenching the reactor, 4.8 g of deionized water was added to perform the hydrolysis at 100 °C for 24 h. Scale bars are 100 nm for (A, D), 20 nm (B, E), 10 nm (G) and 2 nm (H).

from optimized Sn-containing zeolites (Figure S4A). In 24 h, we obtained 1.2, 0.91, and 0.71 $g_{fructose}/g_{catalyst}$ using MIL-101-[GLY], Sn-MWW, and Sn-SPP, respectively. No further glucose conversion and fructose production was observed once the catalyst was removed from the reaction media (Figure S5). The recycling of MIL-101-[GLY] shows an initial loss in activity after the first cycle followed by minor losses up to four cycles. Fructose selectivity remains stable (Figure S4B). The XRD patterns (Figure S6A) and TEM images (Figure S6C) of the reused catalyst, after the 4th run, are very similar to those of the fresh catalyst. Moreover, the structure of the MIL-101 crystal and $Cr(OH)_3$ are intact as confirmed by ADF-STEM (Figure S7). These results indicate that MIL-101-[GLY] microstructure is stable under the reaction conditions. The loss of activity could be attributed to irreversible adsorption of reaction byproducts that partially block the pores. Consistently, Figure S6B shows a small decrease in the Ar-sorption isotherms corroborating this hypothesis.

The MIL-101-nano, which was synthesized with the addition of benzoic acid as modulator shows a typical morphology of MIL-101 crystal and has a similar size as the MIL-101-[GLY] (Figure 2D,E). However, only 24.9% yield of fructose was obtained at 46.2% glucose conversion after 24 h of reaction (Figure 2F) when it was used as the catalyst. Nano-sized $Cr(OH)_3$-[GLY], prepared with the same procedure as that of the MIL-101-[GLY] but without the addition of BDC, is composed of thin layers (Figure 2G,H and Figure S8). As mentioned earlier, the XRD pattern of $Cr(OH)_3$-GLY does not fully agree with that of other $Cr(OH)_3$ materials exhibiting an extra broad peak centered at approximately 17°.[35] This broad XRD peak could be due to the approximately 5.2 Å spacing between $Cr(OH)_3$ layers determined by ADF-STEM (Figure S8). Further studies are required to fully elucidate the structure of $Cr(OH)_3$ made in the presence of glycine. $Cr(OH)_3$-[GLY] provided similar low yield of fructose (Figure 2I) as MIL-101-nano. The glucose conversion and fructose yield only slightly increased when the physical mixture of MIL-101-nano (83 wt%) and $Cr(OH)_3$-[GLY] (17 wt%) was used as the catalyst (Table 1, entry 6).

The NMR experiments with isotopically labeled glucose that are described next revealed a predominantly proton-transfer mechanism for isomerization attributable to $Cr(OH)_3$ with MIL-101 contributing mainly to Lewis acid catalyzed ketalization and to a lesser extent of Lewis acid catalyzed isomerization.

The glucose isomerization mechanism on MIL-101-[GLY] was studied by determining the isotopic identity at the C1 position of the produced fructose with ^{13}C NMR spectroscopy (Scheme S1). The reactions were performed in CD_3OD with [$^{13}C1$, $^{1}H2$]-glucose (glucose with ^{13}C enrichment at C1 position and natural abundance hydrogen at C2 position, denoted as G1 in Scheme S1) or in CH_3OH with [$^{13}C1$,$^{2}H2$]-glucose (glucose with ^{13}C enrichment at C1 position and deuterium enrichment at C2 position, denoted as G2 in Scheme S1). NMR spectra of hydrolyzed products from G1 and G2 are shown in Figures 3A, B, respectively. Figure 3A shows one strong resonance (Singlet I) at 63.84 ppm, which is ascribed to C1 of the [$^{13}C1$,$^{1}H1$]-fructose (β-pyranose configuration), and a triplet (Triplet II) at 63.73 ppm, 63.51 ppm, and 63.29 ppm that results from $^{13}C1$–D J coupling of the [$^{13}C1$,$^{2}H1$]-fructose (β-pyranose configuration).[38,39] Considering that the nuclear Overhauser effect (NOE) leads to the enhancement of signals from H-bearing carbons, relative to D-bearing carbon atoms, the pronounced presence of the

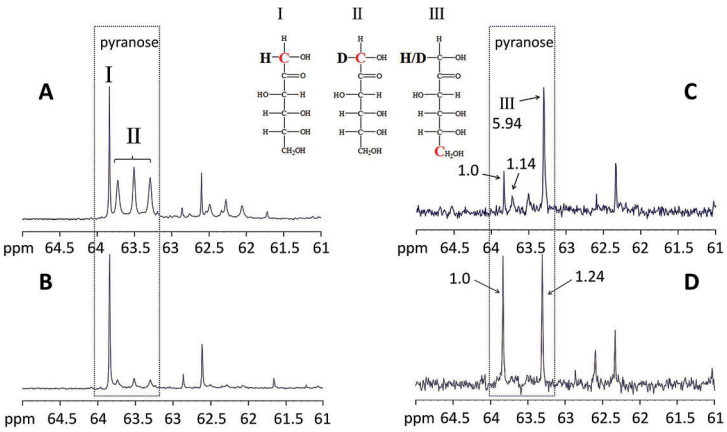

Figure 3. ^{13}C NMR spectra of hydrolyzed products (fructose region) obtained after reactions of A) D-[$^{13}C1$;$^{1}H2$]-glucose (G1) in CD_3OD. B) D-[$^{13}C1$;$^{2}H2$]-glucose (G2) in CH_3OH on MIL-101-[GLY]. Inverse gated coupled quantitative ^{13}C NMR of hydrolyzed products (fructose region) obtained after reactions of C) unlabeled glucose in CD_3OD and D) D-[$^{2}H2$]-glucose in C_2H_5OH on MIL-101-[GLY]. Inset: chemical structures of fructose I—III with the C atoms that give rise to the signals I—III marked in red.

triplet indicates considerable presence of [^{13}C1,^{2}H1]-fructose (fructose shown as formula II in Figure 3) along with [^{13}C1,^{1}H1]-fructose (fructose shown as formula I in Figure 3); suggesting that glucose G1 in CD_3OD was isomerized to fructose in two different ways over MIL-101-[GLY]: 1,2-intramolecular hydride shift to give fructose I and proton transfer mechanisms to give fructose II. Glucose isomerization proceeds primarily via the 1,2-intramolecular hydride shift mechanism on Lewis acid sites like in Sn-containing zeolites (Figure S9A)[40–43] and the proton transfer mechanism proceeds over base catalyst like Na-ETS-4 (Figure S9C).[43,44]

These results were further confirmed by the ^{13}C-NMR spectra of fructose, which were produced from G2 in CH_3OH (See Figure 3B, and compare with Figure S9B and Figure S9D). Here, the triplet is again associated with fructose II but this time corresponds to fructose made by 1,2-intramolecular hydride shift. Moreover, if the two paths were contributing equally, the spectrum of Figure 3B should have been the same as that of Figure 3A. This is not the case, and we can infer that the proton transfer mechanism is the dominant path when MIL-101-[GLY] was used as the catalyst for glucose isomerization. All the reference MIL-101 materials (MIL-101-HF, MIL-101 and MIL-101-nano) show behavior similar to the pure Lewis acid catalysts, while $Cr(OH)_3$-[GLY] behaves like a base catalyst: fructose produced via proton transfer is the dominant product with only trace amount of fructose formed via the hydride shift mechanism (Figure S10).[45]

Inverse gated coupled quantitative ^{13}C-NMR, which suppresses the NOE, was used to further assess the contribution to fructose yield by the two different paths. The integral of Singlet I, which arises from C1 signal of the non-deuterated fructose was quantitated using the integral of Singlet III from the C6 signal of both the non-deuterated fructose and ^{2}H1-fructose (one deuterium at C1 position). If glucose isomerization to fructose proceeds solely via 1,2-intramolecular hydride shift of unlabeled glucose or proton transfer of [^{2}H2]-glucose (glucose with deuterium enrichment at C2 position) in unlabeled alcohol, only non-deuterated fructose would be obtained and the integral of C6 and C1 should be identical.[46] Figure 3C shows the NMR spectrum of the hydrolyzed products from the reaction which was conducted in CD_3OD with unlabeled glucose on MIL-101-[GLY]. It was found that the integral of Singlet I from C1 of non-deuterated fructose, which corresponds to fructose that was produced via 1,2-intramolecular hydride shift was approximately 20% of that of Singlet III (all integrals in Figure 3C were normalized using the integral of Singlet I, and the integral of Singlet III was corrected by the integral at 63.73 ppm due to its overlap with the peak at 63.29 ppm, whose integral is the same as that of the peak at 63.73 ppm as indicated by Figures 3A,B). Figure 3D shows the NMR spectrum of the hydrolyzed products from the reaction, which was done in ethanol starting from [^{2}H2]-glucose (glucose with deuterium enrichment at C2 position). The integral of Singlet I from the C1 of non-deuterated fructose which was formed via proton transfer was approximately 80% of that of Singlet III (the integral of Singlet III in Figure 3D was normalized using the integral of Singlet I). These results demonstrate that approximately 80% of the produced fructose was formed on base-like sites via the proton transfer mechanism and the rest of the fructose was produced on Lewis acid sites of MIL-101 via the hydride shift mechanism.

We propose that the MIL-101-[GLY] catalyst converts glucose into ethanol via a synergistic way and the proximity of chromium hydroxide and Lewis acidic MIL-101 plays a vital role. Specifically, glucose is isomerized to fructose mainly on chromium hydroxide; then the produced fructose is transformed to ethyl fructoside over Lewis acid sites. Therefore, chromium hydroxide and the Lewis acid sites should be close enough to efficiently catalyze the consecutive reactions of glucose isomerization and fructose ketalization. Based on the proton-transfer dominated isomerization, it appears that chromium hydroxide acts as a base catalyst. Further studies including IR spectroscopy of adsorbed CO_2 on MIL-101-[GLY] should be performed in the future to elucidate the type and strength of these sites.[45]

In conclusion, an efficient and reusable MOF-based catalyst containing Lewis acid and base-like chromium hydroxide sites for glucose isomerization in ethanol was synthesized by adding glycine in MIL-101 synthesis. A product distribution of 23.5% glucose, 59.3% fructose, and 2.9% mannose can be obtained over this catalyst, matching the fructose yields achievable by optimized Sn-containing Lewis acidic zeolites.

Acknowledgements

This work was supported as part of the Catalysis Center for Energy Innovation, an Energy Frontier Research Center funded by the U.S. Department of Energy, Office of Science, Basic Energy Sciences under Award DE-SC0001004.

Conflict of interest

The authors declare no conflict of interest.

Keywords: chromium hydroxide · fructose · heterogeneous catalysis · isomerization · metal–organic frameworks

How to cite: *Angew. Chem. Int. Ed.* **2018**, *57*, 4926–4930
Angew. Chem. **2018**, *130*, 5020–5024

[1] H. Zhou, J. R. Long, O. M. Yaghi, *Chem. Rev.* **2012**, *112*, 673–674.
[2] N. Stock, S. Biswas, *Chem. Rev.* **2012**, *112*, 933–969.
[3] T. A. Makal, J. Li, W. Lu, H. Zhou, *Chem. Soc. Rev.* **2012**, *41*, 7761–7779.
[4] N. Rangnekar, N. Mittal, B. Elyassi, J. Caro, M. Tsapatsis, *Chem. Soc. Rev.* **2015**, *44*, 7128–7154.
[5] A. Knebel, B. Geppert, K. Volgmann, D. I. Kolokolov, A. G. Stepanov, J. Twiefel, P. Heitjans, D. Volkmer, J. Caro, *Science* **2017**, *358*, 347–351.
[6] J. Li, J. Sculley, H. Zhou, *Chem. Rev.* **2012**, *112*, 869–932.
[7] D. Hong, Y. Hwang, C. Serre, G. Ferey, J. Chang, *Adv. Funct. Mater.* **2009**, *19*, 1537–1552.

[8] L. Ma, C. Abney, W. Lin, *Chem. Soc. Rev.* **2009**, *38*, 1248 – 1256.
[9] A. Corma, H. Garcia, F. X. Llabrés i Xamena, *Chem. Rev.* **2010**, *110*, 4606 – 4655.
[10] J. Liu, L. Chen, H. Cui, J. Zhang, L. Zhang, C. Su, *Chem. Soc. Rev.* **2014**, *43*, 6011 – 6061.
[11] A. H. Chughtai, N. Ahmad, H. A. Younus, A. Laypkov, F. Verpoort, *Chem. Soc. Rev.* **2015**, *44*, 6804 – 6849.
[12] L. Zhu, X. Liu, H. Jiang, L. Sun, *Chem. Rev.* **2017**, *117*, 8129 – 8176.
[13] S. M. J. Rogge, A. Bavykina, J. Hajek, H. Garcia, A. I. Olivos-Suarez, A. Sepulveda-Escribano, A. Vimont, G. Clet, P. Bazin, F. Kapteijn, M. Daturi, E. V. Ramos-Fernandez, F. X. Llabrés i Xamena, V. Van Speybroeck, J. Gascon, *Chem. Soc. Rev.* **2017**, *46*, 3134 – 3184.
[14] M. B. Majewski, A. J. Howarth, P. Li, M. R. Wasielewski, J. T. Hupp, O. K. Farha, *CrystEngComm* **2017**, *19*, 4082 – 4091.
[15] Z. Hu, D. Zhao, *CrystEngComm* **2017**, *19*, 4066 – 4081.
[16] A. M. Robinson, J. E. Hensley, J. W. Medlin, *ACS Catal.* **2016**, *6*, 5026 – 5043.
[17] F. Vermoortele, B. Bueken, G. Le Bars, B. Van de Voorde, M. Vandichel, K. Houthoofd, A. Vimont, M. Daturi, M. Waroquier, V. Van Speybroeck, C. Kirschhock, D. E. De Vos, *J. Am. Chem. Soc.* **2013**, *135*, 11465 – 11468.
[18] M. J. Katz, J. E. Mondloch, R. K. Totten, J. K. Park, S. T. Nguyen, O. K. Farha, J. T. Hupp, *Angew. Chem. Int. Ed.* **2014**, *53*, 497 – 501; *Angew. Chem.* **2014**, *126*, 507 – 511.
[19] J. E. Mondloch, M. J. Katz, W. C. Isley, P. Ghosh, P. Liao, W. Bury, G. Wagner, M. G. Hall, J. B. DeCoste, G. W. Peterson, R. Q. Snurr, C. J. Cramer, J. T. Hupp, O. K. Farha, *Nat. Mater.* **2015**, *14*, 512 – 516.
[20] J. Jiang, F. Gandara, Y. Zhang, K. Na, O. M. Yaghi, W. G. Klemperer, *J. Am. Chem. Soc.* **2014**, *136*, 12844 – 12847.
[21] K. Sabyrov, J. Jiang, O. M. Yaghi, G. A. Somorjai, *J. Am. Chem. Soc.* **2017**, *139*, 12382 – 12385.
[22] M. Zhao, K. Yuan, Y. Wang, G. Li, J. Guo, L. Gu, W. Hu, H. Zhao, Z. Tang, *Nature* **2016**, *539*, 76 – 80.
[23] X. Li, T. W. Goh, L. Li, C. Xiao, Z. Guo, X. Zeng, W. Huang, *ACS Catal.* **2016**, *6*, 3461 – 3468.
[24] A. Gaona, U. Diaz, A. Corma, *Chem. Mater.* **2017**, *29*, 1599 – 1612.
[25] E. Anderson, A. Crisci, K. Murugappan, Y. Roman-Leshkov, *ChemSusChem* **2017**, *10*, 2226 – 2234.
[26] M. Yabushita, P. Li, T. Islamoglu, H. Kobayashi, A. Fukuoka, O. K. Farha, A. Katz, *Ind. Eng. Chem. Res.* **2017**, *56*, 7141 – 7148.
[27] S. Saravanamurugan, M. Paniagua, J. A. Melero, A. Riisager, *J. Am. Chem. Soc.* **2013**, *135*, 5246 – 5249.
[28] L. Ren, Q. Guo, P. Kumar, M. Orazov, D. Xu, S. M. Alhassan, K. A. Mkhoyan, M. E. Davis, M. Tsapatsis, *Angew. Chem. Int. Ed.* **2015**, *54*, 10848 – 10851; *Angew. Chem.* **2015**, *127*, 10998 – 11001.
[29] L. Ren, Q. Guo, M. Orazov, D. Xu, D. Politi, P. Kumar, S. M. Alhassan, K. A. Mkhoyan, D. Sidiras, M. E. Davis, M. Tsapatsis, *ChemCatChem* **2016**, *8*, 1274 – 1278.
[30] S. Saravanamurugan, A. Riisager, E. Taarning, S. Meier, *ChemCatChem* **2016**, *8*, 3107 – 3111.
[31] G. Akiyama, R. Matsuda, H. Sato, S. Kitagawa, *Chem. Asian J.* **2014**, *9*, 2772 – 2777.
[32] R. Oozeerally, D. L. Burnett, T. W. Chamberlain, R. I. Walton, V. Degirmenci, *ChemCatChem* **2018**, https://doi.org/10.1002/cctc.201701825.
[33] M. Moliner, Y. Roman-Leshkov, M. E. Davis, *Proc. Natl. Acad. Sci. USA* **2010**, *107*, 6164 – 6168.
[34] C. D. Malonzo, S. M. Shaker, L. Ren, S. D. Prinslow, A. E. Platero-Prats, L. C. Gallington, J. Borycz, A. B. Thompson, T. Wang, O. K. Farha, J. T. Hupp, C. Lu, K. W. Chapman, J. C. Myers, R. L. Penn, L. Gagliardi, M. Tsapatsis, A. Stein, *J. Am. Chem. Soc.* **2016**, *138*, 2739 – 2748.
[35] Y. Bai, R. Zheng, Q. Gu, J. Wang, B. Wang, G. Cheng, G. Chen, *J. Mater. Chem. A* **2014**, *2*, 12770 – 12775.
[36] G. Ferey, C. Mellot-Draznieks, C. Serre, F. Millange, J. Dutour, S. Surble, I. Margiolaki, *Science* **2005**, *309*, 2040 – 2042.
[37] A. Herbst, A. Khutia, C. Janiak, *Inorg. Chem.* **2014**, *53*, 7319 – 7333.
[38] Y. Roman-Leshkov, M. Moliner, J. A. Labinger, M. E. Davis, *Angew. Chem. Int. Ed.* **2010**, *49*, 8954 – 8957; *Angew. Chem.* **2010**, *122*, 9138 – 9141.
[39] J. D. Lewis, S. Van de Vyver, Y. Roman-Leshkov, *Angew. Chem. Int. Ed.* **2015**, *54*, 9835 – 9838; *Angew. Chem.* **2015**, *127*, 9973 – 9976.
[40] V. Choudhary, A. B. Pinar, R. F. Lobo, D. G. Vlachos, S. I. Sandler, *ChemSusChem* **2013**, *6*, 2369 – 2376.
[41] G. Yang, E. A. Pidko, E. J. M. Hensen, *ChemSusChem* **2013**, *6*, 1688 – 1696.
[42] I. Delidovich, A. Hoffmann, A. Willms, M. Rose, *ACS Catal.* **2017**, *7*, 3792 – 3798.
[43] R. Bermejo-Deval, M. Orazov, R. Gounder, S. Hwang, M. E. Davis, *ACS Catal.* **2014**, *4*, 2288 – 2297.
[44] J. M. Carraher, C. N. Fleitman, J. P. Tessonnier, *ACS Catal.* **2015**, *5*, 3162 – 3173.
[45] A. Vimont, A. Travert, P. Bazin, J. Lavalley, M. Daturi, C. Serre, G. erey, S. Bourrelly, P. L. Llewellyn, *Chem. Commun.* **2007**, *31*, 3291 – 3293.
[46] C. Yoo, N. Li, M. Swannell, X. Pan, *Green Chem.* **2017**, *19*, 4402 – 4411.

Manuscript received: December 13, 2017
Accepted manuscript online: February 28, 2018
Version of record online: March 22, 2018

